Evaluating process-based sugarcane models for simulating genotypic and environmental effects observed in an international dataset

Jones, M.R.[1,2], Singels, A.[1,2], Chinorumba, S[3]., Poser, C.[4,5], Christina, M.[5,6], Shine, J.[7], Annandale, J.[2], Hammer, G.L.[8]

[1]*South African Sugarcane Research Institute, Private Bag X02, Mount Edgecombe, 4300, South Africa*

[2]*Department of Plant and Soil Sciences, University of Pretoria, Private Bag X20, Hatfield, 0028, South Africa*

[3]*Zimbabwe Sugar Association Experiment Station (ZSAES), P. Bag 7006, Chiredzi, Zimbabwe.*

[4]*Centre de Coopération Internationale en Recherche Agronomique pour le Développement (CIRAD), UPR AIDA, F-34398 Montpellier, France.*

[5]*AIDA, Univ Montpellier, CIRAD, Montpellier, France.*

[6]*Centre de Coopération Internationale en Recherche Agronomique pour le Développement (CIRAD), UPR AIDA, F-97743 Saint-Denis, Réunion, France.*

[7]*Sugarcane Industry Research Committee (SIRC), c/o Sugarcane Growers Cooperative of Florida, 1500 George Wedgworth Way, Belle Glade, Florida 33430, USA.*

[8]*ARC Centre of Excellence for Translational Photosynthesis, Queensland Alliance for Agriculture and Food Innovation, The University of Queensland, Brisbane, Qld 4072, Australia*

Corresponding author: Matthew Jones (matthew.jones@sugar.org.za).

Abstract

Crop modelling has the potential to assist plant breeding by identifying favourable genotypic (G) traits for specific environments (Es). Sugarcane crop models have not been rigorously evaluated against a factorial GxE dataset. It is imperative that models are evaluated in this way before they are applied to plant breeding problems.

Our objectives were to (1) calibrate, (2) assess, and (3) identify weaknesses and recommend improvements to, three sugarcane models, DSSAT-Canegro, Mosicas and APSIM-Sugar, in relation to their predictions of observed E, G and GxE interaction effects in response to abiotic factors (temperature and solar radiation). Data from an international GxE growth analysis trial were used; these consisted of five irrigated experiments at four sites (Belle Glade, Florida, USA; Chiredzi, Zimbabwe; La Mare, Reunion Island; and Pongola, South Africa), with cultivars N41, R570 and CP88-1762. Observed G and E effects on final above-ground dry mass (ADM) yields were explained in terms of seasonal radiation interception (FIPARa) and seasonal average radiation use efficiency (RUEa). Calibration was undertaken where possible by

translating phenotypic parameters derived from observations into model input trait parameter values representing genetic traits.

E and G effects on FIPARa were generally simulated satisfactorily, while GxE interaction effects were poorly predicted due to inadequate responses to temperature. E, G and GxE effects on RUEa were poorly predicted by all models, although data shortcomings (arising from uncertainty regarding date of primary shoot emergence and impacts of lodging) prevented us from making strong conclusions in this regard. Models accurately predicted G differences in RUEa during mid-season biomass sampling periods where data confidence was greater. Although the models were able to predict final ADM yield per G and per E reasonably well, none of the models predicted GxE interaction effects well. All models also under-estimated the variation in RUEa and ADM. Recommendations for experimental protocols for exploring RUEa are made. Our key recommendations for future work to improve models for sugarcane breeding applications are to explore G-specific thermal time base temperatures for germination and canopy development processes, and to improve linkages between carbon availability and canopy development.

Keywords: crop model, genotype, environment, radiation use efficiency, radiation interception, biomass, thermal time, genetic trait, sugarcane

Highlights

- Three crop models were calibrated for three cultivars grown in four countries
- Variability observed in biomass yield was explained via radiation interception and use efficiency
- Genotype and Environment effects on canopy development were accurately predicted
- Genotype by Environment interaction effects in biomass yield were poorly predicted
- G-specific base temperatures for canopy development are needed to improve models.

1. INTRODUCTION

Sugarcane is an important crop grown worldwide, with over 1.84 billion tons of sugarcane grown on 26 million ha worldwide (FAOSTAT, 2017). Sugarcane products include sugar, bio-ethanol, paper, specialist chemicals such as furfural (Gomes et al., 2018), and bio-plastics (e.g. poly-lactic acid, Bonsucro, 2017).

Increasing demand for food, energy and other bio-products, coupled with the limited supply of suitable land and irrigation water, creates the need to maximise sugarcane yields and resource-use efficiency (Hoffman, 2017). Efficient, high-yielding cultivars are produced by sugarcane breeding programmes around the world, but this is resource-intensive and time-consuming (e.g. 11-20 years per cultivar, Zhou, 2013). Sugarcane yields are subject to complex genotype (G; note: acronyms are listed in Table 1) by environment (E) interactions, and process-based crop models capable of

simulating G differences in biologically-realistic ways can support plant breeding by assisting in identifying genotypic traits that confer advantages under particular Es (Hammer and Jordan, 2007; Sexton et al., 2017).

Table 1. Acronyms used in this paper, excluding phenotypic and model trait input parameters (listed in Table 3).

Acronym	Units	Description
ADM	t/ha	Above-ground dry biomass
APE		Average prediction error, defined as the average difference between simulated and observed values
AS		APSIM-Sugar v7.10
DC		DSSAT-Canegro v4.5_C2.2 model
E		Environment or Experiment
FIPAR	%	Fractional interception of photosynthetically-active radiation by green leaves
FIPARa	%	Seasonal average fractional interception of photosynthetically-active radiation by green leaves
G		Genotype
GLAI	m^2/m^2	Green leaf area index
LSD		Least significant difference
MS		Mosicas model (2017 version)
P		Plant crop
PAR	MJ/m^2	Incident photosynthetically-active radiation
$\overline{PP}$		Average value across genotypes of a phenotypic parameter
R1		First ratoon crop
RMSE		Root mean squared error, defined as the square root of the mean squared difference between simulated and observed values
RUEa	g/MJ	Seasonal average apparent radiation use efficiency, calculated as above ground dry biomass at harvest divided by seasonal intercepted photosynthetically-active radiation
RUEo	g/MJ	Model input parameter capturing maximum theoretical radiation use efficiency for a young, disease-free, well-fertilised and well-watered crop
SDM	t/ha	Stalk dry mass
SRAD	MJ/m^2	Incident global solar radiation
T	°C	Daily average air temperature
TMAX	°C	Daily maximum air temperature
TMIN	°C	Daily minimum air temperature
TP_i		Value of a model trait input parameter value for genotype i
$\overline{TP}$'		Average value across all genotypes of an intermediate model trait input parameter whose values were determined via interactive calibration
TT_csFi50	°Cd	Thermal time from crop start to 50% fractional interception of photosynthetically-active radiation by green leaves
WSI		Water stress index, calculated using the DSSAT-Canegro v4.5_C2.2 model
X_{ij}		Value of an observed or simulated variable for genotype i and environment j.
$\overline{X}$		Mean value across all genotypes and environments of an observed or simulated variable

Several process-based sugarcane crop growth simulation models have been developed, including DSSAT-Canegro (Inman-Bamber, 1991; Jones and Singels, 2018; Singels and Bezuidenhout, 2002); APSIM-Sugar (Keating et al., 1999) and Mosicas (Martiné et al., 1999; Martiné and Todoroff, 2004). Biomass accumulation in these models is determined by two key processes: (a) the growth of, and interception of solar radiation by, the sugarcane canopy; and (b) the conversion of intercepted solar radiation into carbohydrates via photosynthesis. Under unstressed conditions, canopy growth is driven by temperature (and additionally by carbohydrate availability from photosynthesis in the case of APSIM-Sugar) and radiation conversion each day is determined by a maximum theoretical radiation use efficiency (defined for a young, disease-free, well-fertilised and well-watered crop, RUEo, g/MJ) and air temperature. Key similarities and differences in simulation approaches between these models are summarized by Jones et al. (2019) and Singels (2014), and model inter-comparison studies have been conducted (Dias and Sentelhas, 2017; Jones et al., 2014; Marin et al., 2015; Thorburn et al., 2014).

The exploration of genotypic trait modelling in sugarcane has been limited (Inman-Bamber et al., 2016; Sexton et al., 2017). Crop model development has generally made use of single standard cultivars – NCo376 for DSSAT-Canegro, Q117 for APSIM-Sugar (Sexton et al., 2017), and R570 for Mosicas (Singels, 2014) – implying that research has mostly focussed on capturing and describing responses to E drivers, rather than G or GxE interaction effects. Models have been calibrated for different Gs (Dias and Sentelhas, 2017; Hoffman et al., 2016; Marin et al., 2011a; A Singels et al., 2010a), but in all cases the range of Es was very limited. Large variation in reported parameter values for the same cultivars between publications casts doubt on the validity of calibration procedures or the reliability of those parameters in representing genetic traits. Singels et al. (2010b) attempted to link sugarcane G trait values (based on sugarcane model concepts) with quantitative trait loci, but for only a single irrigated E. Inman-Bamber et al. (2012) explored GxE interactions of drought-tolerance traits, while Sexton et al. (2017) conducted a trait parameter sensitivity analysis for two contrasting Es, both using APSIM-Sugar, but these studies were largely theoretical with few observed data.

The International Consortium for Sugarcane Modelling (ICSM) launched a project in 2010 to evaluate and improve modelling of sugarcane GxE interactions, in order to support model-assisted breeding. A set of field trials was conducted in four countries, with three cultivars common to all sites (as well as other cultivars grown in fewer of the sites). The rationale behind choosing sites and cultivars from different countries was to maximise potential G, E and GxE interaction effects, thereby permitting better, and perhaps easier, assessment of model abilities to predict growth. The field data for these trials were presented in Jones et al. (2019). In this paper, the authors calculated G-specific phenotypic parameters based on concepts from several crop models, for this international GxE dataset. Clear G differences were identified for parameters (expressed in terms of dominant E drivers, mainly temperature) for photosynthesis and canopy development parameters. Conceptual shortcomings were noted for predicting the timing of primary shoot emergence and onset of stalk growth, which have considerable bearing on yield. Although model concepts were tested in this work, the ability of whole sugarcane models to predict G, E and GxE interaction effects on yield has yet to be evaluated. Given the conceptual shortcomings identified with predicting onset of stalk growth, along with the apparent stability (across Es) of G-specific phenotypic parameters describing photosynthesis and canopy development, the

primary research question for a GxE model assessment should be: to what extent can GxE differences in biomass accumulation be predicted by models calibrated to reflect our knowledge of G control over canopy development and photosynthesis?

Rigorous evaluation of any sugarcane crop model for a factorial 'GxE' study, has not, to our knowledge, been conducted. It is essential that the prediction performance for G, E and GxE interaction effects of widely-used sugarcane models is established before they can be applied to assist plant breeding. Identification of weaknesses in such models could also lead to improvements that make models more suitable for supporting breeding.

The overall goal of this study was to evaluate three sugarcane models' capabilities for simulating genotypic differences in crop development and growth in different environments, using an international growth analysis data set consisting of three genotypes grown in four countries. It was hypothesised that by setting model trait input parameters based on observed G-specific phenotypic data, current models of crop response to abiotic factors (mainly temperature and radiation) would be able accurately to predict observed G and GxE effects. Specific objectives were to:

- Calibrate three sugarcane crop models for three genotypes, by estimating model trait input parameter values controlling canopy development and radiation use efficiency, using phenotypic data from Jones et al. (2019);
- evaluate model performance for predicting G, E and GxE interaction effects on canopy development, radiation use efficiency and aboveground biomass accumulation (using the same dataset);
- assess model strengths and weaknesses in simulating genetic control of physiological processes; and recommend model improvements for supporting sugarcane breeding.

2. METHODS

2.1 Experiments

Eight growth analysis experiments were conducted: plant and first ratoon crops of cultivars N41, R570 and CP88-1762 grown at Belle Glade (Florida, USA), Chiredzi (Zimbabwe), La Mare (Reunion Island, France) and Pongola (South Africa). Plant crops were established on adjacent fields. Field 1 ("plant crop") was sampled in the first year up until 12 months' age; the second field ("first ratoon crop") cut back after 12 months (approximately) and was sampled in the second year. This two-field approach prevented inconsistent ratoon age consequences of destructive in-field sampling and subsequent mid-season regrowth in the preceding plant crop. Plots were nine rows (13.5 m) wide and 11 m long (≈ 150 m^2), and each treatment was replicated four times.

Non-destructive measurements (replicated three times) of shoot population were taken at 2-4 week intervals, and PAR interception was measured using quantum line sensors 2-7 times (depending on the experiment) mostly during the partial canopy phase. Destructive samples were taken at 3, 6, 9 and 12 months after crop start; 18 m^2 samples (replicated four times) were cut and weighed. Sub-samples of 3 m^2 were then divided into biomass fractions, weighed, oven-dried and weighed again; dry matter contents from the sub-samples were then multiplied by the original 18 m^2 aerial fresh

mass sample weights to determine dry mass values for different above-ground biomass components.

It was intended that all crops would be well-fertilised and irrigated sufficiently to avoid water stress. In practice, significant water stress could not be avoided for the Chiredzi and La Mare plant (P) crops, and the Pongola first ratoon (R1) crop. This paper focusses primarily on the unstressed experiments.

The experiments are fully described in Jones et al. (2019).

2.2 Environmental characterisation

Each experiment (equivalent to environment (i.e. one season at one site), both designated "E") was characterised following the methods described in Jones et al. (2019). To summarise: averages of mean daily temperature, daily maximum temperature, daily minimum temperature, a simulated water stress index (WSI, based on the ratio of potential evapotranspiration to potential root water uptake) and the sum of SRAD (daily incident global solar radiation, MJ/m^2/d), were calculated for several phenological phases (germination, tillering, germination and tillering together, the stalk growth phase, and the season as a whole). The WSI and phenological phases were calculated using the DSSAT-Canegro v4.5_C2.2 (Jones and Singels, 2018) model with NCo376 input parameters.

2.3 Data analysis

Observed and simulated apparent radiation use efficiency (RUEa, g/MJ) were calculated as above-ground dry biomass (ADM, t/ha) at final harvest divided by seasonal canopy-intercepted PAR. The energy content of PAR was assumed to be 50% of observed SRAD. Observed daily fractional interception of photosynthetically-active radiation (FIPAR, %) values were interpolated between observations using a fitted model based on the Canesim model canopy algorithm (Singels and Donaldson, 2000), using the procedure described in Jones et al. (2019). Observed and simulated average seasonal fractional PAR interception (FIPARa, %) were calculated as the sum of daily FIPAR multiplied by PAR, divided by total PAR. The thermal time from crop start to 50% FIPAR (TT_csFi50, °Cd) was calculated from fitted daily FIPAR values for each G and E (for observed and simulated data).

G, E and GxE interaction effects were evaluated using the following additive linear model:

$$X_{ij} = \bar{X} + G_i + E_j + GE_{ij} \quad (1)$$

where X_{ij} is observed or simulated FIPARa, RUEa or ADM, $\bar{X}$ is the grand mean value calculated over all environments and genotypes, G_i is the average value for genotype i, and E_j is the average value for environment j:

$$G_i = \left(\frac{1}{n_E} \sum_{j=1}^{n_E} X_{ij} \right) - \bar{X} \quad (2)$$

$$E_j = \left(\frac{1}{n_G} \sum_{i=1}^{n_G} X_{ij} \right) - \bar{X} \quad (3)$$

where n_E is the number of environments and n_G is the number of genotypes. *GEij* was calculated by rearranging eq. (1) and substituting the other terms.

Simulated values of FIPARa, RUEa and ADM were compared with observed values, as were G, E and GxE interaction effects on these. Model performance was quantified in terms of the slope and intercept of the linear regression between simulated and observed values, and the coefficient of determination (R^2).

Differences in observed ADM between Gs and Es were tested for significance by analysis of variance followed by post hoc pairwise comparisons using the Fisher 'least significant difference' (LSD), calculated using the R Agricolae package (de Mendiburu, 2019). It was not possible to calculate LSD values for RUEa and FIPAR as these were derived from treatment means.

2.4 Models and simulation setups

Simulations were conducted with three models: DSSAT-Canegro v4.5_C2.2 ("DC"), Mosicas (2017 version, "MS"); and APSIM-Sugar v7.10 ("AS").

Location and management-related model inputs for the simulations are listed in Table 2. Soil descriptions are shown in Table S2 in the Supplementary Online Material. The DSSAT v4.6.1 'SBuild' software (Wilkens et al., 2004) was used to estimate soil hydraulic properties from texture and bulk density observations, for all models. Soil (rooting) depth set to maximum sampling depth or 120 cm (whichever was greater). Where sampling was conducted to a shallower depth, the properties of the deepest sample were extended to 120 cm depth.

Table 2. Start and harvest dates, and initial bud population used in simulations.

				Planting density (buds/m^2)			
Country, site and location	**Crop class**	**Start date (Y-m-d)**	**Harvest date (Y-m-d)**	**N41**	**R570**	**CP88-1762**	**Irrigation type**
USA, Belle Glade. 26°39'02"N; 80°38'08"W; 5 m a.s.l	Plant	2013-12-12	2015-01-04	6	6	5	Automatic (to avoid stress)
	Ratoon	2015-01-23	2016-01-26	8	8	8	
Zimbabwe, Chiredzi. 21°02'01.95"S, 31°36'58.52"E, 420 m a.s.l.	Plant	2013-10-30	2014-11-26	10	9	12	Furrow (recorded amounts)
	Ratoon	2015-06-03	2016-06-03	22	18	16	Overhead sprinkler (recorded amounts)
Reunion, La Mare. 20°57'0"S; 55°18'0"E; 70 m a.s.l.	Plant	2015-02-25	2016-02-23	8	8	8	Overhead sprinkler (recorded amounts)
	Ratoon	2016-01-18	2017-01-25	14	8	18	
South Africa, Pongola. 27°24'0"S; 31°35'0"E; 308 m a.s.l.	Plant	2014-03-25	2015-03-24	12	12	12	Overhead sprinkler and drip (recorded amounts)
	Ratoon	2015-03-24	2016-03-23	12	8	10	

The soil at Belle Glade is mostly organic material and the standard pedotransfer functions for estimation of hydraulic characteristics do not apply. We used a predefined soil released with DSSAT v4.5 ('Lauderhill muck', code BGIGEP2013, described as a hyperthermic Lithic Haplosaprist), and modified the thicknesses of the deepest two layers so that the soil profile depth matched the profile depth reported by the data cooperator at that site (179 cm). Rather than extending the bottom layer to depth, the second-deepest was extended, as the deepest layer was (originally) defined to be near-impermeable.

The soil description reported in Jones (2013) was used for the Pongola simulations. All simulations were initialized with 100% plant-available soil water content.

The MS model was run with the 'MOSICASCERESb' water balance option enabled. Penman-Monteith short grass reference evapotranspiration (ETo, mm/day) was calculated with the R 'Evapotranspiration' library (Guo et al., 2017).

Recorded irrigation applications were used for simulations at La Mare, Pongola and Chiredzi. Irrigation application data were not recorded for the Belle Glade experiments, as irrigation is undertaken by adjusting water table depth at that site. For the Belle Glade experiments only, models were set up to apply enough water to avoid water stress.

2.5 Estimation of model input parameter values

2.5.1 General considerations

The basic approach was to calibrate models for the following processes, in order (based on the sequence of calculations during each simulated day in the models): duration of germination, canopy development (including leaf and tiller appearance where applicable), biomass accumulation, biomass partitioning (including timing of onset of stalk growth). The data used for calibrating the model were all from the international GxE trial described by Jones et al. (2019). This comprised (1) directly observed values for shoot population, stalk length, leaf number and leaf area index, fractional interception of photosynthetically active radiation, stalk dry mass, and above-ground dry mass; and (2) derived data values (names and definitions are listed in Table 3, data are shown in Table S3 in the Supplementary Online Material), termed hereafter in this text as 'phenotypic parameters'. These phenotypic parameter values describe observations, but are not model inputs themselves. The term 'trait parameter', by contrast, refers to a crop model trait input parameter, and the names of these are italicised in the text. Trait parameter values were determined according to a hierarchy of approaches:

1. '*A priori*' method: in advance of running any crop models, from the G-means (for unstressed experiments only, unless otherwise stated) of the phenotypic parameter values. In some cases, mathematical transformation of the phenotypic parameters was necessary to match specific model input parameter definitions. This approach was preferred and used wherever phenotypic parameter definition were sufficiently similar to model trait parameter definitions.
2. 'Interactive' method: via trial and error, in two steps: 1), by changing trait parameter values, running simulations, and then assessing model accuracy by comparing simulated and observed values of relevant variables, in order to simulate E effects as accurately as possible; then 2) by imposing relative G

values of related observed phenotypic parameters in order to capture G differences.

3. 'model default' method: where observations were not available to support either *a priori* or interactive methods, default (standard) model trait parameter values were used for each model (NCo376 for DSSAT-Canegro, R570 for Mosicas and Q117 for APSIM-Sugar).

Equivalent parameter values were set for the radiation extinction coefficient (all models), maximum number of green leaves (DC and AS), and the short grass reference evapotranspiration multiplier (DC and MS), to minimise confounding.

Input parameter values determined using the *a priori* approach were calculated and input into the models before attempting interactive calibration of remaining parameters. For interactive calibration, for DC and MS (models with no dynamic feedback between biomass accumulation and leaf area development) the order in which trait parameter values were determined followed the order of daily rate calculations in which these trait parameters are used within the models. For the AS model, where biomass accumulation feeds back on leaf area development, every combination of model trait parameter values was assessed in parallel, avoiding feed-forward effects arising from sequential interactive calibration.

For trait parameters determined via interactive calibration, observed G differences for phenotypic parameters *RUEmax* (maximum apparent radiation use efficiency across biomass sampling periods, g/MJ), *TT_csFi50* and *STKPF* (fraction of daily above-ground dry biomass increments allocated to stalks), were imposed on initial calibrated values of the relevant model trait parameters. In the explanations below, names for initial parameter values are appended with an apostrophe (e.g. *ruemax'* as the intermediate value name for *ruemax*) to indicate their intermediate nature. The basic form of this 'imposition' of G effects follows equation (4):

$$TP_i = \overline{TP'} * \frac{PP_i}{\overline{PP}} \qquad (4)$$

where TP_i is a model trait input parameter value, $\overline{TP'}$ is the average of intermediate interactively-determined trait input parameter values for all Gs, PP_i is the related phenotypic parameter value for genotype *i*, and $\overline{PP}$ is the average of the phenotypic parameter values for all three Gs.

The same trait parameter values were used for plant and ratoon crops except for two germination-related input parameters: *taldebtt* (thermal time duration for germination, °Cd) for MS and *shoot_lag* (thermal time duration from crop start to start of linear coleoptile, °Cd) for AS.

The input parameter value derivations are summarized in Table 3.

2.5.2 DSSAT-Canegro calibration

The *a priori* method was used to estimate DC trait parameter values for timing of germination, leaf appearance and start of stalk growth, the duration of tillering, final stalk population and biomass partitioning.

Interactive calibration for the DC model was performed in a specific order based on the sequence of calculations performed in the model each day. For each trait parameter in the sequence, default (NCo376) values were used for as-yet uncalibrated trait parameters. The calibration sequence was as follows:

1. *TAR0'* (maximum unstressed tiller appearance rate per primary shoot, shoots/shoot/°Cd, before imposition of G differences): the DC model calculates the timing of secondary shoot emergence using temperature and FIPAR > 70% (a dynamic feedback mechanism linking tillering with leaf-related trait parameters and growing conditions via radiation interception). *TAR0'* was determined by minimizing differences between simulated and observed shoot population for the first 2 months of each season (FIPAR generally less than 70%), minimising the potentially confounding effects of dynamic feedback.
2. *LER0* (maximum unstressed leaf elongation rate, cm/°Cd) was calibrated by minimising differences in GLAI, over the first 3-4 months of each cropping season. The age cutoff was to ensure that leaf number had not yet reached the point where leaf length is limited by the maximum leaf area size parameter MXLEAFAREA (cm^2), which would have confounded the calibration.
3. *MXLEAFAREA* was then calibrated by minimising differences between simulated and observed GLAI, focussing on observations from 6 months age onward.
4. *TAR0*: after calibrating *TAR0'*, *LER0* and *MXLFAREA* for all three Gs, the final values of *TAR0* for each G were determined by imposing relative differences in observed TT_csFI50 on the average (of the three Gs) TAR0' values, using eq. (4).
5. *MAXPARCE'* (defined as gross assimilate produced per unit PAR intercepted for a young healthy crop growing under ideal temperature and water status conditions, g/MJ, before imposition of G differences) was determined by minimising differences between simulated and observed ADM accumulation.
6. *MAXPARCE*: after calibrating *MAXPARCE'* for all three Gs, relative differences in RUEmax (a phenotypic parameter from Jones et al. (2019), defined as the maximum radiation use efficiency calculated from ADM and PAR measurements across biomass sampling periods) were then imposed on the average MAXPARCE' using eq. (4) to determine per-G *MAXPARCE* values.

2.5.3 Mosicas calibration

For the MS model, the *a priori* method was used to determine values for trait parameters controlling germination timing, canopy development (*laicroi'*, green leaf expansion rate per unit thermal time, $m^2/m^2/°Cd$) and biomass partitioning.

Interactive calibration was conducted for trait parameters in the following sequence:

1. *laicroi* was determined by revising the initial values of laicroi' to minimise differences between simulated and observed TT_csFi50.
2. *ruemax'* (maximum photosynthetically-active radiation use efficiency, defined as growth respiration-net[1] assimilate produced per unit PAR intercepted for a young healthy crop growing under ideal temperature and water status conditions, g/MJ, before imposition of G differences) was calculated by minimising differences between simulated and observed ADM.
3. *ruemax* values were determined after other trait parameter values had been calculated and input into the models, for all Gs. G differences in the phenotypic parameter RUEmax were imposed on *ruemax',* following eq (4), to determine *ruemax* values per G.

[1] Assimilate produced after losses to growth respiration, but before losses to maintenance respiration.

Where the use of default values was necessary, standard values for ratoon crops were used for both P and R1 crops, as we had more confidence in these.

2.5.4 APSIM-Sugar calibration

The *a priori* calibration approach was used to calculate trait parameter values governing germination rate, leaf appearance rate and onset of stalk growth. The stalk biomass partitioning fraction parameter *cane_fraction* was initially set to 0.80 g/g for all Gs on the basis of the STKPF phenotypic parameter values, as was done for DC and MS, but this had the effect of starving the canopy of biomass and resulted in considerably underestimated and unrealistic radiation interception and yields.

Trait parameter *tillerf_leaf_size* (the 'tillering factor', a multiplier intended to emulate the effect of tillering on green leaf area index (GLAI, m^2/m^2)) and *leaf_size* (maximum unstressed leaf area per leaf, cm^2) were considered to be mutually compensating, so *tillerf_leaf_size* was set to default (Q117) values and only *leaf_size* was changed in the calibrations. Following this, the *leaf_size* parameter should be interpreted as a G index of canopy size (including tillering effects) rather than leaf size per se. Note that we assumed the same (Q117 plant crop) *tillerf_leaf_size* values for P and R1 crops, as we attributed faster shoot population growth in R1 crops to greater primary shoot population via the initial seed density simulation trait parameter.

The AS model restricts canopy expansion to carbohydrate availability, requiring simultaneous calibration of input parameters for leaf size, biomass accumulation and biomass partitioning, respectively: *leaf_size*, *rue* and *cane_fraction* (see Table 3 for definitions). For each G, the AS model was run for all Es, for numerous combinations of parameter values ranging around those for the standard (cultivar Q117). Every combination of parameter sets from the three Gs was then determined and the absolute average prediction error (APE, defined as the average difference between observed and simulated values) for ADM was calculated across Gs. Input parameter set combinations that had the same G ranking for *rue* and *cane_fraction* respectively as that of related phenotypic parameters RUEmax and STKPF (Jones et al., 2019), were shortlisted. From these, the input parameter set combination with the lowest absolute APE for ADM across Gs was selected to arrive at values for *leaf_size*, *rue'* and *cane_fraction* per G.

Finally, observed G differences in RUEmax were then imposed on *rue'* (using eq (4)).

Table 3. Derived phenotypic and model trait parameter names, definitions, and method of estimation used in this study, for three models: DSSAT-Canegro v4.5_C2.2, Mosicas 2017 and APSIM-Sugar v7.10. Values in bold text indicate derived parameters calculated in Jones et al., 2019; brief explanations for how these parameters were determined are provided, and definitions are provided at the first use. Data for unstressed experiments only were used unless otherwise specified.

Parameter name	Definition, units	Estimation Method	Comment
Model evaluation variables			
POPN	Shoot population, shoots/m^2	Counts per 10 m row length	Jones et al., 2019
GLAI	Green leaf area index, m^2/m^2	Determined destructively with leaf area meters	
FIPAR	Fractional interception of photosynthetically-active radiation, %	Measured with line quantum sensors	
ADM	Above-ground dry biomass, t/ha	Determined destructively from 18 m^2 samples	
SDM	Stalk dry mass, t/ha	Determined destructively from 18 m^2 samples	
Derived phenotypic parameters			
TT_EM50	Thermal time requirement from crop start to the 50th percentile primary shoot emergence for P and R1 crops, °Cd	Thermal time (TT10[1]) from crop start to 50% primary shoot emergence (**TT_EM50**, °Cd) was either recorded or visually assessed from tiller population observations.	All experiments data were used.
PI	The phyllochron interval is the thermal time required for the production of one fully expanded leaf, °Cd	Determined as the slope of linear regression of leaf number against thermal time (TT10), for the first 30 leaves.	
PFINAL	Final shoot population, stalks/m^2	The average of the last three observations of shoot population	
PPOP	Peak shoot population, shoots/m^2	Maximum observed shoot population value.	
RUEmax	Maximum apparent radiation use efficiency, defined as above-ground dry biomass accumulated per unit intercepted photosynthetically-active radiation (g/MJ)	Apparent radiation use efficiency was calculated from the above-ground dry biomass increment and estimated intercepted photosynthetically active radiation for each of four biomass sampling periods, and the maximum value was selected.	
ADM_OSG	Above-ground dry biomass at the start of stalk growth, t/ha	X-intercept of linear regression of observed **SDM** against **ADM**.	
STKPF	Fraction of daily above-ground dry biomass increments allocated to stalks, t/t	Slope of linear regression of **SDM** and **ADM**.	

TT_OSG	Cumulative thermal time ($TT10^1$) since 50% primary shoot emergence at start of stalk growth, °Cd	Used a linear regression of TT10 and **ADM** to predict cumulative TT10 when ADM=**ADM_OSG**.	
TT_Fi50	Thermal time ($TT16^2$) from 50% shoot emergence to 50% canopy cover (in terms of photosynthetically-active radiation interception), °Cd	The Canesim canopy equation was fitted (by optimising numerical input parameter values) to observed **FiPAR** observations to 'fill in' between observations; this was then solved for $TT16^2$ nearest 50% predicted FiPAR.	
FIPARa	Seasonal average fractional interception of photosynthetically-active radiation	Calculated as the sum of daily intercepted photosynthetically-active radiation (PAR, MJ/m^2) divided by total incident PAR. Daily intercepted PAR was calculated using a fitted Canesim canopy equation to interpolate between observations, and observed daily solar radiation values.	
DSSAT-Canegro trait parameters			
TTPLNTEM, TTRATNEM	Thermal time requirement from crop start to first primary shoot emergence for P and R1 crops respectively, °Cd	**TT_EM50** was converted from $TT10^1$ to $TT16^2$, and 98 °Cd was subtracted to account for the TT difference between first and 50th percentile primary shoot according to eq 7 of Jones and Singels (2018) [Supplementary Online Material].	All experiments data were used.
PI1, PI2	Leaf phyllocron intervals 1 and 2, °Cd	'*a priori*' determination from **PI**, by multiplying the ratio of default NCo376 values for *PI1* or *PI2* to the 30-leaf average NCo376 phyllocron interval, by **PI**.	
POPTT16	Final shoot population, stalks/m^2	Used values of **PFINAL.** No data transformations were required.	
TTPOPGROWTH	Thermal time from primary shoot emergence to end of tillering, °Cd	Cumulative $TT16^2$ on the date of **PPOP**, minus *TTPLNTEM* or *TTRATNEM* depending on crop class.	
TAR0	Shoot appearance rate per primary shoot per unit $TT16^2$, shoots/shoot/°Cd	Initially calibrated interactively against observed shoot population data (**POPN**), then finalised to match per-G simulated and observed thermal time from crop start to 50% **FiPAR** (see text)	
MXLFAREA	Maximum area per leaf at leaf number 15, cm^2	Initially calibrated interactively against observed green leaf area index (**GLAI**) and then finalised to	

LER0	Leaf elongation rate per unit TT10[1], cm/°Cd	match simulated and observed average fractional interception of photosynthetically-active radiation (see text).	
EXTCFST	Minimum (young crop) canopy photosynthetic radiation extinction coefficient	Average value from literature (0.65)	Luo et al., 2013
EXTCFN	Maximum (leaf #20) canopy photosynthetic radiation extinction coefficient	Average value from literature (0.65)	Luo et al, 2013.
MAXPARCE	Maximum photosynthetically-active radiation use efficiency, defined as gross assimilate produced per unit PAR intercepted for a young healthy crop growing under ideal temperature and water status conditions, g/MJ	Initially determined interactively against observed aerial dry biomass (**ADM**) and finalised by imposing relative **RUEmax** values (see text).	
CHUPIBASE	TT from primary shoot emergence to onset of stalk growth, °Cd	TT10[1] accumulated between simulated date of emergence of first primary shoot (determined by *TTPLNTEM* or *TTRATNEM*) and estimated date of onset of stalk growth (as determined from **SDM** and **ADM** observations)	
STKPFMAX	Maximum stalk partitioning fraction, t/t	**STKPF** used without transformation. No G differences were found so a single value was used for all three Gs	
Mosicas trait parameters			
taldebtt	Thermal time from crop start to 50% primary shoot emergence for P and R1 crops, °Cd	Translated **TT_EM50** by converting from TT10[1] to thermal time calculated with a base temperature of 14 °C.	All experiments data were used.
kcmax	Sugarcane crop evaporation coefficient, mm/mm	Set to 1.15 for consistency with DSSAT-Canegro	Jones & Singels, 2018
laitb	Base temperature for thermal time accumulation for canopy development, °C	Base temperature from the thermal time measure which had the lowest relative variation in **TT_Fi50** between experiments.	Jones et al., 2019; Jones & Singels, 2018

laicroi	Green leaf expansion rate per unit thermal time, $m^2/m^2/°Cd$	Solved (iteratively) for G-specific values of *laicroi* that closely matched corresponding **TT_Fi50** values, by using the model's canopy development equation to predict GLAI, and FIPAR predicted using the Beer's Law equation. Finalised to match per-G simulated and observed thermal time from crop start to 50% FIPAR (see text)	
laiwksen	GLAI water stress senescence coefficient	Set to the default value for ratoon crops.	
ke	PAR extinction coefficient	Average value from literature (0.65)	Luo et al, 2013.
ruemax	Maximum photosynthetically-active radiation use efficiency, defined as growth respiration-net assimilate produced per unit PAR intercepted for a young healthy crop growing under ideal temperature and water status conditions, g/MJ	Determined interactively against observed **ADM** and then finalised by imposing relative **RUEmax** (see text).	
ptigdeb	ADM threshold to commence stalk growth, g/m^2	**ADM_OSG** units translated from t/ha to g/m^2	
ptigfin	Final (maximum) biomass partitioning fraction to stalk, t/t	The value for *ptigfin* (0.90 t/t) is essentially a guess; *ptigdec* was then calculated such that the average **SDM** partitioning fraction for the observed range of **ADM_OSG** to average final **ADM** (5-48 t/ha) was equal to **STKPF**.	Ptigfin = 0.90 may be unrealistically high.
ptigdec	Biomass partitioning to stalk shape coefficient		
APSIM-Sugar trait parameters			
shoot_lag	Thermal time delay required for germination, from crop start to start of linear coleoptile growth (elongation of shoot from sett towards the soil surface), °Cd	**TT_EM50** was converted to $TT9^3$, and TT9 required for coleoptile elongation (187.5 and 62.5 °Cd respectively for P and R1 crops) was subtracted.	
y_node_app_rate	Leaf phyllocron intervals for leaves 1, 20, 30 and 40, defined as the thermal time required to produce one fully expanded leaf, °Cd	Default (Q117) values were multiplied by a relative phyllocron interval value, calculated as **PI** divided by the average phyllocron interval for the first 30 leaves of Q117.	
green_leaf_no	Maximum number of green leaves per shoot, leaves/shoot	Set to DSSAT-Canegro model default of 12 leaves/shoot for consistency.	Inman-Bamber, 1994

leaf_size	Maximum (unstressed) leaf area per leaf, for leaves 1, 14 and 20, mm^2	Determined interactively in combination with *rue* and *cane_fraction* against observed **ADM** (detailed explanation in text)	
extinction_coef	Canopy extinction coefficient for global radiation	Estimated for global radiation from published photosynthetically-active radiation extinction coefficient.	Luo et al., 2013 Jovanovic and Annandale, 1998
rue	Maximum global radiation use efficiency, defined as net (after respiration) above-ground biomass produced per unit global radiation intercepted for a young healthy crop growing under ideal temperature and water status conditions, g/MJ	Determined interactively in combination with *leaf_size* and *cane_fraction* against observed **ADM** (detailed explanation in text)	
tt_emerg_to_begcane	Thermal time from primary shoot emergence to onset of stalk growth, °Cd	TT9[3] accumulated between simulated date of emergence (assuming bud depths of 150 and 50 mm for P and R crops) and estimated date of onset of stalk growth (as determined from **SDM** and **ADM** observations)	
cane_fraction	Stalk partitioning fraction, defined as the fraction of dry biomass increments partitioned to stalks in the stalk growth phase, t/t	Determined interactively in combination with *rue* and *leaf_size* against observed **ADM** (detailed explanation in text)	

[1]TT10: cumulative thermal time from crop start calculated using a base temperature of 10 °C, with optimal and upper temperatures as specified in Jones and Singels, 2018.

[2]TT16: cumulative thermal time from crop start calculated using a base temperature of 16 °C, with optimal and upper temperatures as specified in Jones and Singels, 2018.

[3]TT9: cumulative thermal time from crop start calculated using a base temperature of 9 °C, with optimal and upper temperatures are specified in Keating et al., 1999.

2.6 Assessment of model performance

The key research question we set out to answer was: can models predict G and GxE interaction effects on ADM accumulation and its components? The models were forced, via calibration, with knowledge of observed G and E effects on canopy development- and biomass accumulation phenotypic data. This section describes the evaluation of the calibrated models. Models were evaluated with the same dataset used for calibration. This might overestimate overall model performance, but ensures that G and E effects on crop processes are simulated as accurately as possible, permitting meaningful evaluation of GxE interaction effects.

Models were assessed in two broad ways:

1. A 'traditional' model assessment, where time-series observations were statistically compared with corresponding simulated values, done primarily to establish a baseline indication of calibration quality, compatible and comparable with published calibration/validation statistics.
2. Analysis of variance to assess models' abilities to predict G, E, and GxE interaction effects of key variables.

Model accuracy was measured with the following statistical parameters that quantified the accuracy of simulated time series values of green leaf area index (GLAI, m^2/m^2), fractional interception (FIPAR, %) of PAR, ADM and stalk dry mass (SDM, t/ha): the slope and intercept of the linear regression between simulated and observed values, R^2; root mean squared error (RMSE, defined as the square root of the mean squared difference between simulated and observed values); and APE.

Model performance improvements by calibrated cultivars over standard model calibrations were assessed by comparing N41 observations with simulations run using standard model trait parameter sets (representing cultivar NCo376 for DC, R570 for MS and Q117 for AS; N41 observations were chosen as none of the models had been developed/calibrated with this cultivar).

3. RESULTS

3.1 Environmental characterization

Environmental conditions varied by E and growth phase (Table 4).

Table 4. Number of days, average daily: mean (T), maximum (TMAX) and minimum (TMIN) temperature; sum of solar radiation (SRAD); and average daily water stress index (WSI), for growth phases as defined by the DSSAT-Canegro model standard parameters. WSI is low for germination because there is no transpiration before emergence.

Experiment	Days	T (°C)	TMAX (°C)	TMIN (°C)	SRAD (MJ/m^2)	WSI
Germination						
La Mare, P	24	26.4	30.1	22.8	489	0.00
La Mare, R1	10	27.5	31.3	23.7	247	0.00
Pongola, P	34	22.1	28.4	15.8	552	0.01
Pongola, R1	13	23.7	29.3	18.2	224	0.00
Belle Glade, P	50	18.2	23.7	12.6	563	0.00
Belle Glade, R1	31	16.0	22.4	9.6	493	0.00
Chiredzi, P	24	27.9	34.1	21.7	493	0.01
Chiredzi, R1	24	17.8	26.2	9.4	394	0.00
Tillering						
La Mare, R1	60	27.2	30.8	23.7	1207	0.09
Pongola, P	121	18.6	26.6	10.6	1688	0.04
Belle Glade, P	93	21.2	27.4	15.0	1783	0.01
Belle Glade, R1	77	23.6	29.2	17.9	1598	0.06
Chiredzi, R1	96	20.8	28.9	12.7	1703	0.03
Pre-stalk growth phase (germination and tillering phases together)						
La Mare, R1	71	27.3	30.9	23.7	1454	0.07
Pongola, P	156	19.4	27.0	11.8	2241	0.03
Belle Glade, P	144	20.1	26.1	14.2	2346	0.01
Belle Glade, R1	109	21.4	27.2	15.5	2091	0.04
Chiredzi, R1	121	20.2	28.4	12.0	2097	0.03
Stalk growth						
La Mare, R1	300	23.8	27.6	20.1	5866	0.04
Pongola, P	200	23.4	29.4	17.4	3891	0.15
Belle Glade, P	224	24.6	29.9	19.3	4228	0.03
Belle Glade, R1	257	25.2	30.1	20.3	4365	0.08
Chiredzi, R1	243	25.9	32.3	19.5	5303	0.11
Post-emergence						
La Mare, R1	360	24.4	28.1	20.7	5090	0.05
Pongola, P	321	21.6	28.3	14.8	3061	0.11
Belle Glade, P	317	23.6	29.2	18.0	3511	0.02
Belle Glade, R1	334	24.8	29.9	19.7	3727	0.08
Chiredzi, R1	339	24.5	31.3	17.6	4284	0.09
Seasonal						
La Mare, R1	372	24.5	28.2	20.8	7320	0.05
Pongola, P	357	21.7	28.4	14.9	6132	0.10
Belle Glade, P	369	22.8	28.4	17.3	6573	0.02
Belle Glade, R1	367	24.0	29.2	18.9	6456	0.07
Chiredzi, R1	365	24.0	31.0	17.0	7401	0.08

Water stress (due to irrigation supply issues) was found to be too severe at Chiredzi P, La Mare P and Pongola R1, and these Es were excluded from analysis other than that for germination. Simulations showed that MS and AS predicted more severe water stress than DC at Chiredzi R1, La Mare R1 and Pongola P. Pongola P revealed end-of-season water stress, attributed to deliberate drying-off, standard practice for enhancing sucrose content prior to harvest.

Belle Glade P and R1, Chiredzi R1 and Pongola P started and ended the season relatively cool, with warm (Pongola) or hot (Belle Glade) mid-season conditions; La Mare R1 was hot at the start and end of the season, with a warm mid-season. Minimum temperatures were higher at La Mare R1 than other Es. Seasonal solar radiation was highest at Chiredzi R1 and La Mare R1, and lowest at Pongola P.

3.2 Model trait parameter values

Model trait parameter values following calibration are listed in Table 5.

Table 5. Model cultivar parameter values for DSSAT-Canegro v4.5_C2.2, Mosicas, and APSIM-Sugar v7.10: standard values and those derived through calibration from phenotypic data.

Parameter	Units	Standard[1] value	Calibrated values		
			N41	R570	CP88-1762
DSSAT-Canegro					
TTPLNTEM	°Cd	150	149	175	159
TTRATNEM	°Cd	100	9	102	16
TAR0	shoots/shoot/°Cd	*0.0236*	0.016	0.010	0.012
TTPOPGROWTH	°Cd	600	886	875	736
TTPOP16	shoots/m^2	13.3	12.4	8.7	10.4
PI1, PI2	°Cd/leaf	69, 169	85, 208	96, 236	82, 200
LER0	cm/°Cd	*0.180*	0.250	0.400	0.300
MXLFAREA	cm^2	*360*	200	515	320
EXTCFST		0.58	0.65	0.65	0.65
EXTCFN		0.84	0.65	0.65	0.65
MAXPARCE	g/MJ	*5.40*	4.23	4.27	4.50
CHUPIBASE	°Cd	1050	1157	1090	1024
STKPFMAX	t/t	0.75	0.80	0.80	0.80
Mosicas					
Kcmax	mm/mm	*1.25*	1.15	1.15	1.15
taldebtt (P)	°Cd	*200*	314	346	327
taldebtt (R1)	°Cd	*40*	151	274	160
Laitb	°C	*12*	16	16	16
Laicroi	-	*0.00415 (R1 crops)*	0.0087	0.0094	0.0108
Laiwksen	-		0.0187	0.0187	0.0187
Laiwksen	-	*0.0187 (R1 crops)*	0.0187	0.0187	0.0187
Ke	-	*0.48*	0.65	0.65	0.65
Ruemax	g/MJ	*2.54 (R1 crops)*	2.73	2.79	2.93
Ptigdeb	g/m^2	*200 (P)*	590	580	440

		500 (R1)			
Ptigdec	-	*1.25*	3.0	3.0	3.0
Ptigfin	t/t	*0.78*	0.90	0.90	0.90
APSIM-Sugar					
shoot_lag (P)	°Cd	250	296	345	315
shoot_lag (R1)	°Cd	100	210	408	225
y_node_app_rate	°Cd	80, 105, 125, 150	103, 136, 162, 194	117, 154, 183, 220	99, 131, 156, 187
green_leaf_no	leaves/shoot	13	12	12	12
leaf_size	mm^2/leaf for leaves 1, 14 and 20	1500, 55000, 55000	1650, 60500, 60500	1050, 38500, 38500	1050, 38500, 38500
extinction_coef		0.35	0.46	0.46	0.46
Rue	g/MJ	1.80 (P); 1.65 (R1)	1.30	1.40	1.50
tt_emerg_to_begcane	°Cd	1900	1045	1002	910
cane_fraction	t/t	0.70	0.74	0.76	0.76

[1] –Standard values are provided by model developers for standard cultivar

3.3 Calibration accuracy

The 'traditional' evaluation (Table 6) reveals similar performance between the models. Predictions of GLAI were relatively poor, but did not greatly reduce FiPAR and ADM prediction performance. MS, DC and AS predicted ADM with RMSEs of 6.45, 6.81 and 8.63 t/ha. Calibration considerably improved most model performance statistics compared to standard cultivars (Table 6), particularly for ADM and SDM.

*Table 6. Model evaluation statistics for non-stressed experiments, for calibrated and uncalibrated models. 'Sign.' refers to the statistical significance of the R^2 statistic: *** (P<0.001), ** (P<0.01), * (P<0.05). "Calibrated" used calibrated cultivars and compared with corresponding simulated and observed values; "Default" refers to model default parameters (i.e. standard cultivars: NCo376 for DSSAT-Canegro, R570 for Mosicas and Q117 for APSIM-Sugar), where simulated values were compared with N41 observations.*

Cultivar	Variable	APE	RMSE	Slope	Intcpt.	R^2	Sign.
	DSSAT-Canegro v4.5_C2.2						
Calibrated	Green leaf area index (m^2/m^2)	0.19	1.52	0.49	1.36	0.24	**
Calibrated	PAR Frac. Int. (%)	2.96	11.97	0.83	9.65	0.83	***
Calibrated	Aerial dry biomass (t/ha)	-0.03	6.81	1.04	-0.99	0.89	***
Calibrated	Millable stalk dry mass (t/ha)	1.40	5.91	0.99	-1.12	0.84	***
Default	Green leaf area index (m^2/m^2)	-0.89	1.40	0.53	0.64	0.47	*
Default	PAR Frac. Int. (%)	-6.72	14.13	0.75	13.46	0.85	***
Default	Aerial dry biomass (t/ha)	-8.40	10.93	0.79	-1.17	0.93	***
Default	Millable stalk dry mass (t/ha)	-5.94	7.38	0.82	-1.48	0.94	***

	Mosicas						
Calibrated	Green leaf area index (m^2/m^2)	2.11	2.87	0.36	1.03	0.34	***
Calibrated	PAR Frac. Int. (%)	-0.77	16.32	0.64	26.21	0.86	***
Calibrated	Aerial dry biomass (t/ha)	0.05	6.45	1.06	-1.67	0.90	***
Calibrated	Millable stalk dry mass (t/ha)	0.65	5.00	0.99	-0.44	0.88	***
Default	Green leaf area index (m^2/m^2)	-1.38	2.96	0.13	1.89	0.10	ns
Default	PAR Frac. Int. (%)	36.50	46.72	0.35	59.75	0.32	*
Default	Aerial dry biomass (t/ha)	8.21	10.80	1.11	6.13	0.88	***
Default	Millable stalk dry mass (t/ha)	9.43	11.96	1.19	7.61	0.72	***
	APSIM-Sugar						
Calibrated	Green leaf area index (m^2/m^2)	0.34	1.45	0.54	1.10	0.35	***
Calibrated	PAR Frac. Int. (%)	-1.82	17.27	0.72	21.33	0.65	***
Calibrated	Aerial dry biomass (t/ha)	0.12	8.63	0.95	1.14	0.82	***
Calibrated	Millable stalk dry mass (t/ha)	3.45	6.65	0.84	0.08	0.88	***
Default	Green leaf area index (m^2/m^2)	-2.68	2.97	0.46	0.05	0.66	**
Default	PAR Frac. Int. (%)	-3.60	13.50	0.78	13.06	0.78	***
Default	Aerial dry biomass (t/ha)	-9.99	14.65	0.71	0.36	0.81	***
Default	Millable stalk dry mass (t/ha)	-4.93	8.60	0.70	2.15	0.88	***

Figure 1-Figure 3 show simulated (after calibration) and observed FiPAR, ADM and SDM time series values, for all three models. The similarity in model performance is clear. FiPAR predictions were generally similar between the models, except at La Mare R1 where FiPAR was greatly underestimated by AS, and FiPAR at Pongola shows a greater separation between the models compared to other Es and variables.

Statistical parameters generally indicate a high degree of accuracy – equivalent to the best published sugarcane model performance (as reported in Jones et al., 2018).

Statistics for simulated ADM yields at harvest, per G, are summarised in Table 7. The R^2 values for simulated vs observed ADM at harvest were weak for DC and MS ($R^2 \approx 0.40$) and stronger for AS ($R^2 \approx 0.67$).

*Table 7. Model performance statistics per cultivar, for **above-ground dry biomass** (t/ha) values at harvest. "Slope" and "Y_Int" are the slope and y-intercept respectively of linear regression between simulated vs observed values.*

Model	Cultivar	APE	RMSE	Slope	Y_Int	R^2	P-value
DSSAT	N41	-1.54	7.07	1.59	-25.3	0.73	0.06
	R570	-3.69	9.48	1.36	-13.3	0.48	0.20
	CP88-1762	2.49	9.05	0.28	36.3	0.03	0.79
Mosicas	N41	-1.52	10.65	0.70	15.1	0.17	0.49
	R570	-4.24	9.30	1.42	-15.2	0.55	0.15
	CP88-1762	-1.74	6.18	0.88	7.4	0.47	0.20
APSIM	N41	1.83	9.43	2.05	-52.8	0.45	0.21
	R570	-0.84	6.88	2.31	-64.0	0.97	0.00
	CP88-1762	3.20	6.07	0.90	2.4	0.60	0.12

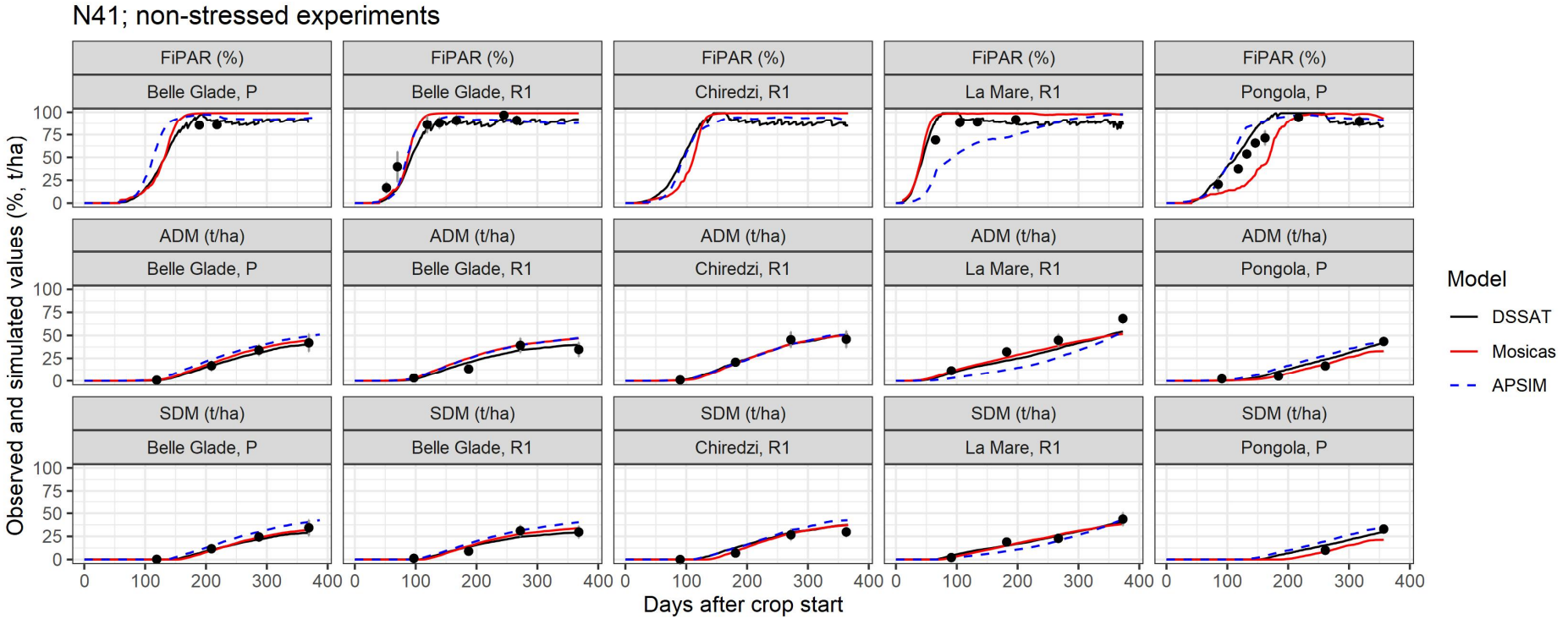

*Figure 1. Simulated (using three models, DSSAT-Canegro, Mosicas and APSIM-Sugar) and observed (black filled circles) fractional interception of photosynthetically-active radiation (FiPAR, %), above-ground dry biomass (ADM, t/ha) and stalk dry mass (SDM, t/ha), for cultivar **N41**.*

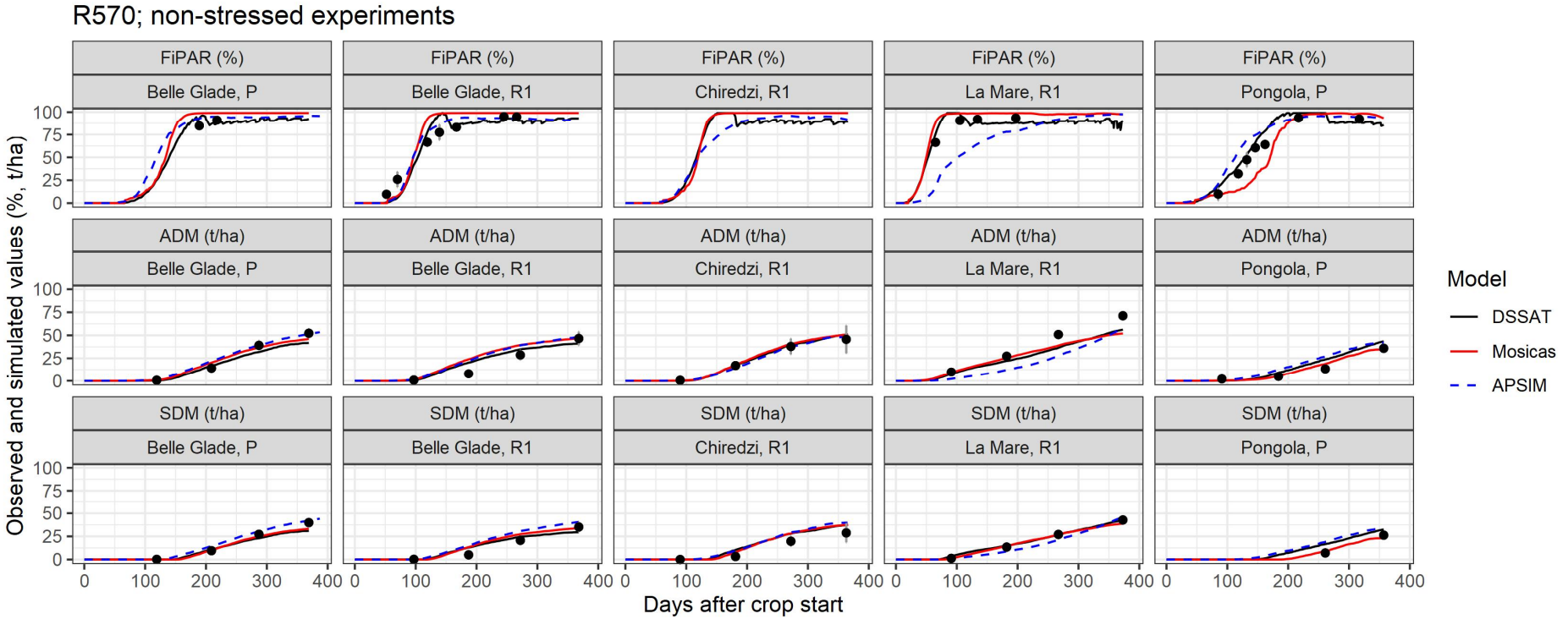

*Figure 2. Simulated (using three models, DSSAT-Canegro, Mosicas and APSIM-Sugar) and observed (black filled circles) fractional interception of photosynthetically-active radiation (FiPAR, %), above-ground dry biomass (ADM, t/ha) and stalk dry mass (SDM, t/ha), for cultivar **R570**.*

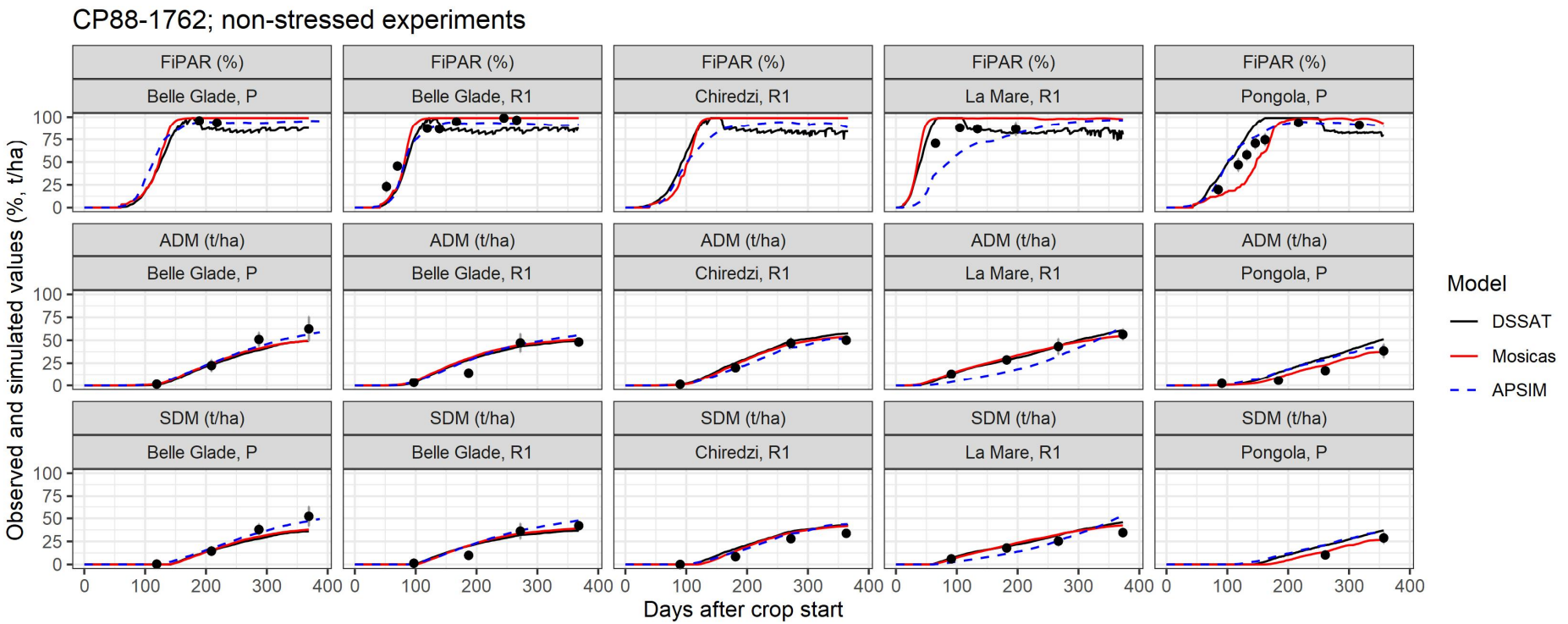

*Figure 3. Simulated (using three models, DSSAT-Canegro, Mosicas and APSIM-Sugar) and observed (black filled circles) fractional interception of photosynthetically-active radiation (FiPAR, %), above-ground dry biomass (ADM, t/ha) and stalk dry mass (SDM, t/ha), for cultivar **CP88-1762**.*

3.4 Observed and simulated G, E and GxE interaction effects

3.4.1 Radiation interception

Crops grown at La Mare R1 showed highest observed FIPARa due to rapid canopy development in response to very warm conditions at crop start (Figure 4, and Table S4 in the Supplementary Online Material). By contrast, Belle Glade P had the lowest FIPARa, due to relatively cool conditions at the start of the season. The DC model correctly predicted the highest and lowest FIPARa Es, while MS correctly predicted the E with the highest FIPARa. Analysis (Figure 4) revealed that E effects were captured well by DC and MS, and poorly by AS.

CP88-1762 showed higher FIPARa than N41 and R570 at all Es except La Mare R1 (indicating a GxE interaction effect). N41 and R570 had similar FIPARa for all Es except Belle Glade R1, where N41 lodged more severely than R570. G effects were shown to be accurately captured by all three models (Figure 4).

DC correctly predicted that CP88-1762 was the highest-ranking G for FIPARa in three Es, but incorrectly predicted N41 (instead of R570) as the highest-ranked G at La Mare R1. The MS model correctly predicted CP88-1762 as the highest-ranked G in three Es, except for La Mare R1 where R570 was incorrectly ranked lowest instead of highest. AS ranked CP88-1762 highest at all Es (with N41 in three Es), and was also unable to predict R570 as the highest-ranking G for FIPARa at La Mare R1. Although the DC and MS models simulated G and E effects accurately, the analysis (Figure 4) revealed that none of the models was able to simulate accurately the observed GxE interaction effects on canopy development.

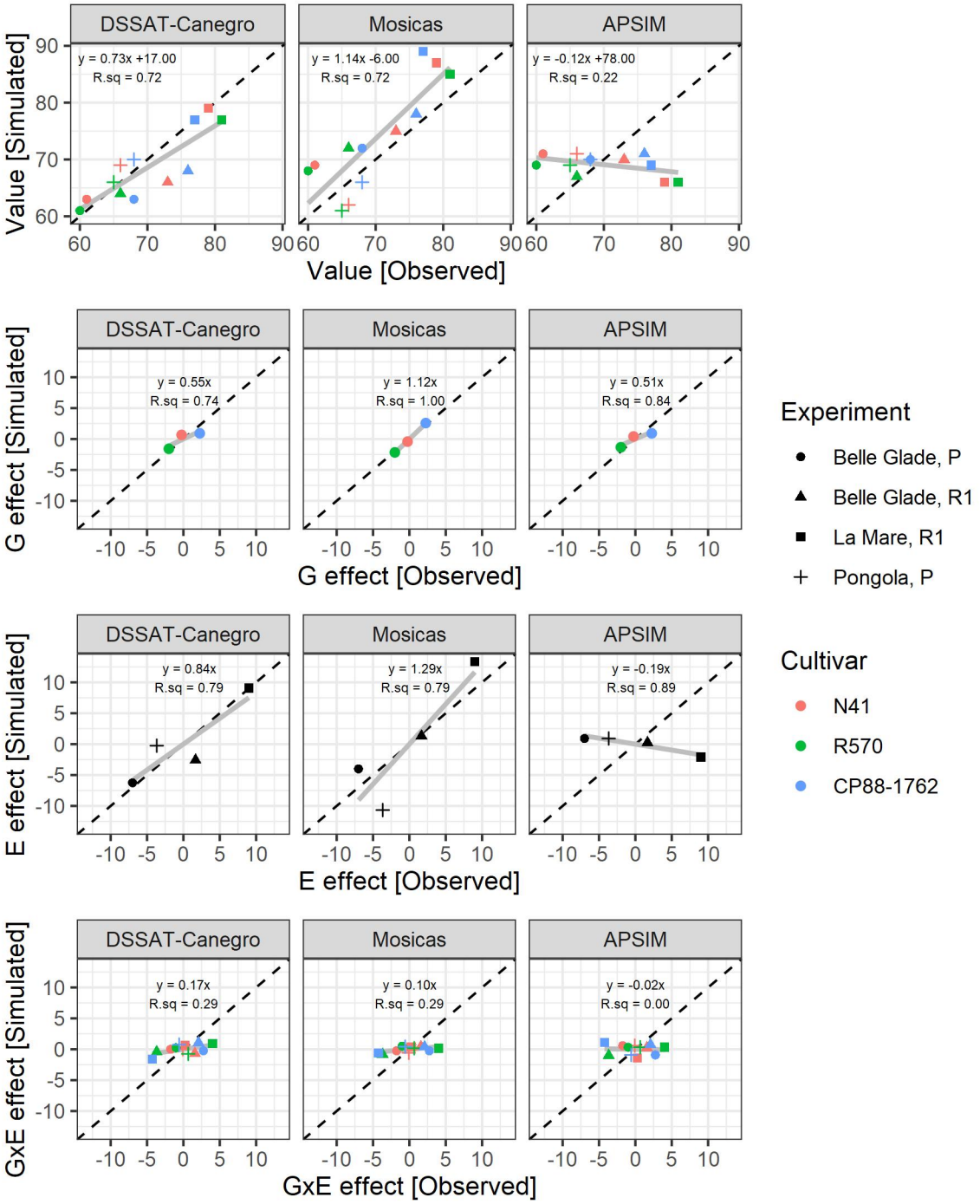

Figure 4. Scatter plot of simulated vs observed G, E and GxE interaction effects on seasonal average interception (%) of photosynthetically-active radiation (FIPARa, %), for each combination of cultivar G and experiment E, for three models.

3.4.2 Radiation use efficiency (RUEa)

Observed RUEa (Figure 5, and Table S5 in the Supplementary Online Material) was highest at Belle Glade P followed by La Mare R1, Pongola P and lastly Belle Glade R1, where lodging occurred.

E variation in RUEa (the difference between maximum and minimum values, expressed as a percentage of the grand mean) was greatly underestimated by the models (4-9% compared to 16-20%). The Es with highest- and lowest-RUEa were not

predicted correctly by any of the models. The AS model captured E differences in RUEa most accurately, but the relationship between observed and simulated RUEa values was still rather weak (R^2 = 0.35, Figure 5). The analysis shown in Figure 5 confirms that E effects on RUEa were poorly predicted by all models.

Variation in observed RUEa between Gs was ≈ 10-20 %. RUEa was highest for CP88-1762 at Belle Glade P, R570 at La Mare R1, and N41 at Pongola P. The low observed value for N41 at Belle Glade R1 was attributed to particularly severe, early lodging.

G variation in simulated RUEa was much lower than observed for DC (7-10%), MS (2-4%) and AS (2-3%). All models predicted highest RUEa for CP88-1762 in all Es, although MS and AS in some cases predicted R570 RUEa values very similar to those of CP88-1762). Simulated G rankings per E in RUEa (Table S5 of Supplementary Online Material) matched RUEo trait parameter values (Table 5). There were generally poor correlations (R^2 = 0.03, 0.02 and 0.24 for DC, MS and AS respectively) between observed and simulated RUEa per G and E. DC and AS greatly over-estimated the G effects for CP88-1762, while MS appeared to capture the G effects on RUEa reasonably well.

RUEa GxE interaction effects (Figure 5) were found to be poorly predicted by all models.

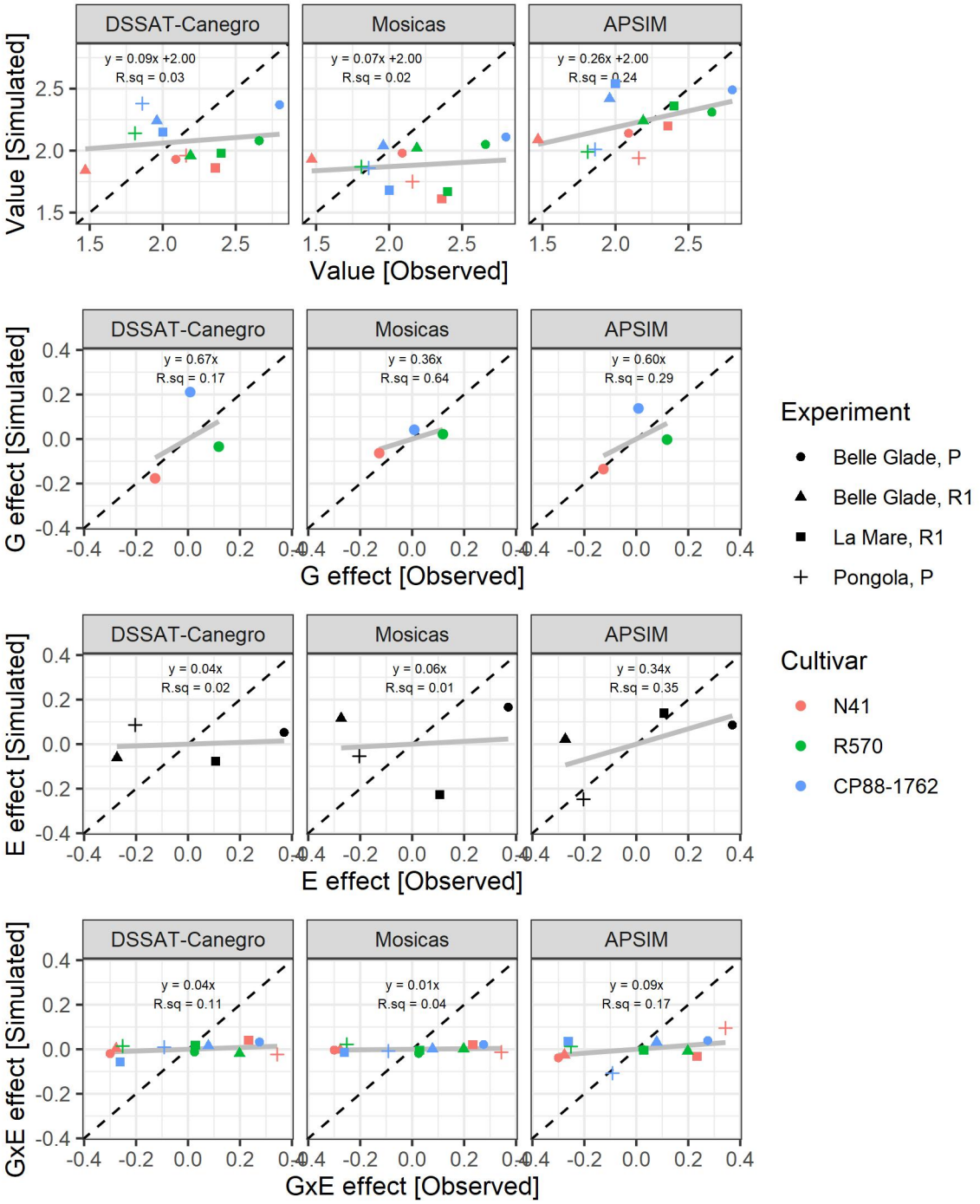

Figure 5. Scatter plot of simulated vs observed G, E and GxE interaction effects on seasonal apparent RUE (RUEa, g/MJ), for each combination of cultivar G and experiment E, for three models.

3.4.3 Above-ground dry biomass accumulation

The range in observed E mean ADM was 26 t/ha (53% of the grand mean) with La Mare R1 and Pongola P showing the highest and lowest values respectively (Figure 6, and Table S6 in Supplementary Online Material). This is ascribed to a combination of: (1) 20% greater fractional radiation interception (Figure 4; Table S5, Supplementary Online Material), attributed to higher temperatures primarily during germination and

tillering (Table 4); (2) 20% higher SRAD; and (3) 16% higher RUEa (Figure 4;Table S5, Supplementary Online Material).

Models under-predicted the observed range of E variation, with DC = 29%, MS = 38% and AS = 20%. Nevertheless, all three models correctly predicted the highest-yielding E, and MS and AS also correctly predicted the lowest-yielding E. AS stands out as having correctly predicted the E-mean ADM rankings for the three Es that were significantly different (Belle Glade P, La Mare R1 and Pongola P), and E effects on ADM yield (Figure 6) were predicted most accurately by this model.

Severe lodging was recorded at Belle Glade R1, and Pongola P crops experienced water stress for several weeks before final harvest due to irrigation being withheld. These may have had differential G impacts and so confound analysis of GxE influences on ADM. FIPAR was not recorded at Chiredzi R1. Consequently, the strongest comparison that can be made is Belle Glade P and La Mare R1.

CP88-1762 produced the highest ADM yield at Belle Glade P, ascribed to high FIPARa (Figure 4; Table S4, Supplementary Online Material) and high RUEa (Figure 5; Table S5, Supplementary Online Material) compared to other Gs. At La Mare R1, however, CP88-1762 produced the lowest yield. This change in G ranking between the two Es matches the change in G rankings of FIPARa and RUEa. G effects on ADM yield appear to be reasonably well-predicted by the models. It should however be noted that although observed E and GxE interaction effects were statistically significant ($p<0.001$ and $p<0.01$ respectively), observed G effects were not (Jones et al., 2019, supplementary online material).

The DC model predicted highest ADM yields for CP88-1762 at every E (Table S6 in Supplementary Online Material). DC predicted very similar ADM values for R570 and N41 at all Es. The AS model predicted CP88-1762 as the top-yielding G at all Es. All models therefore correctly predicted the top-yielding G (CP88-1762) at Belle Glade, and failed to predict the top-yielding G (R570) at La Mare R1. The prediction of GxE interaction effects in ADM was poor by all models, with DC faring least poorly. The AS model E effects more accurately than DC, and despite its poorer GxE interaction effects predictions, its predictions of final ADM were more accurate overall than DC (and MS).

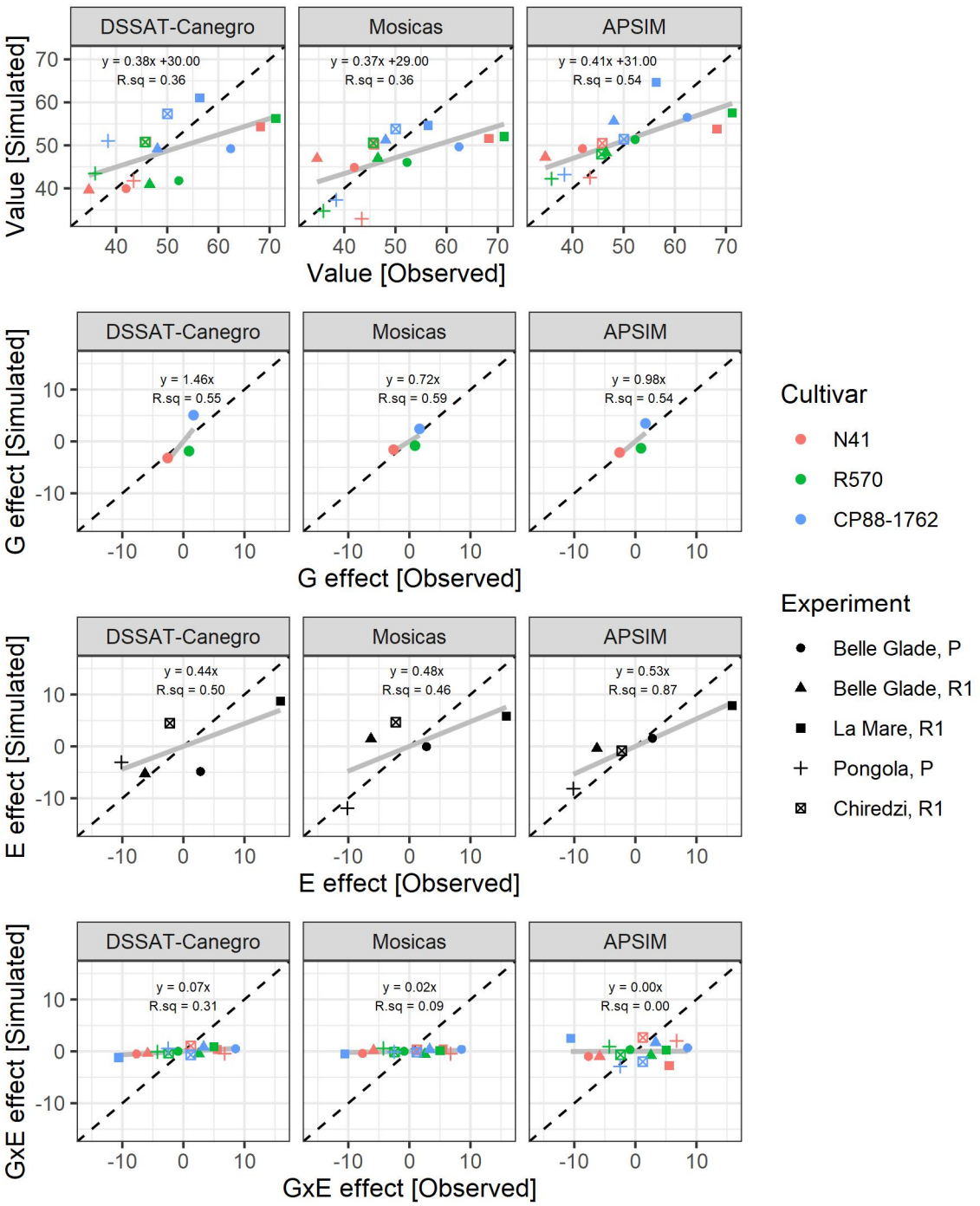

Figure 6. Scatter plot of simulated vs observed additive G, E and GxE interaction effects on final harvest above-ground dry biomass (t/ha), for each combination of cultivar G and experiment E, for three models.

4. DISCUSSION

4.1 Model calibration

The ‘a priori’ calibration approach, of deriving model trait parameter values directly from low-level phenotypic observations, may be more appropriate than interactive calibration (including automatic optimisation, particularly against high level phenotypic observations, e.g. final stalk yield) for model-assisted breeding applications that demand biological realism in simulated plant processes (Hammer and Jordan, 2007). Another advantage of the *a priori* calibration approach is that the sequence of parameter calibration is irrelevant.

The order in which trait parameters are determined using the interactive calibration approach can, however, be important, because of feed forward and feedback effects. This was managed in this study by matching the calibration sequence with the order in which the trait parameters are used in the models, at least for the DC and MS models which have few internal feedbacks between processes and clear feed-forward effects.

For the AS model it was necessary to follow a ‘brute force’ approach, by which every permutation of values for three model trait parameters was tested in parallel, to avoid impacts of sequential calibration and thereby ensuring repeatability. Computationally, this was manageable for the limited number of parameters and experiments; for larger datasets this might not be practical.

The imposition of observed G differences on interactively-determined model parameters – effectively using prior knowledge of G effects to augment automated parameter estimation – appears to be reasonably robust and more appropriate than simply accepting optimised parameter values.

Model calibration and validation are generally based on comparisons of equivalent directly-observed values such as leaf area index, leaf and shoot numbers, yield and biomass partitioning ratios and their simulated equivalents. Less commonly, a model rate or state variable might be compared with a data variable computed from direct observations – e.g. a soil water deficit factor regulating photosynthesis and relative carbon exchange rates between irrigated and dry treatments (Singels et al., 2010c). Model calibration and evaluation was assisted in this study by comparing simulated and observed TT_csFi50, FIPARa and RUEa, which (for these models anyway) must be derived for both observed and simulated datasets. In order for simulated yield to be correctly and *realistically* accumulated, these intermediate ’integrated’ sub-traits must be correct, and so these can serve as “checks and balances” for the simulation of the formation of final yield. It is recommended that similar approaches are followed in future multi-G simulation studies.

It was not clear that calibration would have had much impact on model performance, particularly under well-watered conditions, given the small performance improvements to calibration reported (for example) by Thorburn et al. (2014) and Jones et al. (2014) for the AS and DC models respectively. The substantial improvement in model performance following calibration in this study (Table 6) increased confidence in the credibility of the models for capturing genotypic effects, and justified further analysis of these effects. This also permitted critical assessment of standard model parameter values.

Some of the parameter values calibrated deviated substantially from default values, and it was not possible to conduct an independent validation of these with the available data. While many of these new values should be used with caution, some can be used with more confidence:

- The radiation extinction coefficients (DC: *EXTCFN* and *EXTCFST*; MS: *Ke*; AS: *extinction_coef*) used in this study were based on independent published values. Dias et al. (2019) increased the AS model *extinction_coef* to 0.65, also recognising that the default value is too low, although 0.65 is considerably higher than the value used in the present study (0.46) for SRAD interception. Increasing this parameter value requires, all else being equal, a reduction in the RUEo parameter value (i.e. DC: *MAXPARCE*, MS: *ruemax*; AS: *rue*) in order to avoid over-estimating ADM accumulation. The calibrated RUEo parameter values for both the DC *(MAXPARCE*) and AS (*rue*) models were 10-20% lower than defaults. Dias et al. (2019) did not change *rue* following their increase in *extinction_coef*, although an RUE-reducing growth slow-down feature was introduced.
- The thermal time from emergence to the onset of stalk elongation (DC: *CHUPIBASE*; AS: *tt_emerg_begcane*) was found to be too low for both DC and AS The recommendation for reducing this value (rather than simply accepting this as a G difference between Q117 and the cultivars studied here) is based on two pieces of evidence: (1) the AS simulation of these experiments using Q117 parameter values underestimated FIPARa and ADM, but predicted SDM accurately, suggesting the need to reconsider the relevant parameter values; (2) consistent with the reduction in *tt_emerg_to_begcane* (from 1900 to ≈ 1000 °Cd) found in this study, Dias and Sentelhas (2017) and Dias et al (2019) reported considerably reduced values for this parameter (1025 and 493 °Cd respectively).

4.2 Canopy development (FIPARa)

Canopy development differences between Es were associated with temperature differences. The DC and MS models were able to differentiate FIPARa reasonably well between Es.

CP88-1762 showed quicker canopy development and higher FIPARa than R570 for three Es with relatively low temperatures (Belle Glade P and R1, Pongola P) during the pre-stalk growth phase (Table 4). In contrast, R570 had higher FIPARa than CP88-1762 at La Mare R1 where temperature during this phase was much higher (27.3 compared to 19.4, 20.1 and 21.4 °C). This seems a clear indication that CP88-1762 is better adapted to low temperatures than R570.

Despite the poor prediction of GxE interaction effects, the DC and MS models simulated FIPARa reasonably accurately overall (simulated vs observed linear regression slope = 0.73 (DC) and 1.14 (MS), R^2 ≈ 0.70 (both)).

4.3 Radiation use efficiency (RUEa)

RUEa was, on average, 2.15 g/MJ, about 25% lower than the equivalent RUEa values reported by Robertson et al. (1996) under high-potential conditions in Australia (noting that interception of global rather than photosynthetically-active radiation was originally measured in that study), but similar to the mean RUEa (2.21 g/MJ) reported by Donaldson et al. (2008) for several cultivars grown at Pongola.

Observed RUEa differences between Es are clearly evident, but cannot be easily related to E drivers. None of the models were able to distinguish RUEa accurately between Es. Pongola P had lower RUEa than the other Es (excluding heavily-lodged Belle Glade R1). As this was the coolest E overall (average 21.6 °C post-emergence compared with ≈ 24-25 °C for other Es, Table 4), this may be evidence for RUE temperature sensitivity in the 20-25 °C range. Donaldson et al. (2008) found that RUEmax increased from ≈1.5 g/MJ at 21 °C to ≈2.5 g/MJ at 25 °C for irrigated crops of NCo376, N25 and N26 at Pongola. Mild/transient water stress (where cold and dry conditions coincide, e.g. Pongola) and even the ratio of diffuse to direct solar radiation (Sinclair and Muchow, 1999) may also account partly for these outcomes.

Observed G differences per E in RUEa correlated strongly with observed ADM yields ($r=0.73$, $p < 0.05$), but did not relate well to RUEo model parameter inputs or to the E drivers tested. Seasonal RUEa results may have been confounded by errors in interpolating observed FIPAR during the partial canopy phases, and by lodging and water/nutrient stresses closer to final harvest. Subsequent analysis (results not shown) did find agreement between RUEo trait parameter values and RUEa per G calculated during the 3-6 and 6-9 biomass sampling periods. CP88-1762 had been assigned the highest RUEo based on the RUEmax phenotypic parameter findings of Jones et al. (2019); the analysis in the present paper suggests that R570 ought to have been assigned the maximum RUEo value instead, with CP88-1762 lying between N41 and R570. This discrepancy is attributed to shortcomings in the sensitivity of the RUE algorithms (or cardinal temperature inputs) in the models, resulting in overall over-estimation of CP88-1762 RUE, rather than scaling up RUE when conditions were favourable.

None of the models were able accurately to predict G rankings in RUEa per E, nor were any able to predict the GxE interaction effects accurately. Hoffman et al. (2018) reported stable and accurate G rankings in DC-simulated SDM yields for four fully-irrigated crops at Pongola, attributed to independently-determined stable RUEo values. Jones et al. (2019) found evidence for small but significant G differences in *RUEmax*. G-specific values for RUEo model trait parameters have been reported by Marin et al. (2011b), Dias and Sentelhas (2017) and Coelho et al. (2020); GxE rankings in RUEa were not revealed in these results, however. In contrast, RUEo parameter values were not changed during model calibration by Marin et al. (2015) and Dias et al. (2019). Donaldson et al. (2008) reported consistent G-specific reductions in growth rates (i.e. RUEa) in response to seasonal variation in temperature, although Dias et al. (2019) were able to predict G-specific growth slowdown in APSIM-Sugar using generic leaf number-linked RUEo multipliers and without changing RUEo. The influence of G differences, and temperature in the range 20-30 °C, on RUE, are not fully resolved and warrant further investigation.

4.4 Recommendations for future work

It is recommended that canopy development algorithms be refined for better support *of in silico* crop improvement research. The GxE interaction effect on FIPARa appears to strongly determine ADM yields ($r=0.57$, $p < 0.05$), indicating that improving models' abilities to predict GxE differences in FIPARa will also improve their predictions of GxE interactions in ADM. No clear benefits to the detailed DC model canopy were noted. This may have been due to limitations in the data. The evidence from this study

suggests that model performance gains for predicting yield GxE interactions in fully-irrigated sugarcane crops can be made, even using a simple model of canopy development (e.g. in the MS model), by using G-specific base temperatures for canopy development (and perhaps photosynthesis as well).

The value of a canopy model that couples leaf area development with biomass availability (as in the AS model) was not clearly demonstrated here. Deeper exploration of GxE interaction mechanisms may however require a rigorous examination of carbon supply and demand and assessment (or addition) of these linkages in crop models. Source-sink dynamics are unavoidable in nature, so including these mechanisms in the models adds to their biological realism, and likely holds potential both increasing simulation accuracy in general, but also specifically for improving definitions and values of G trait parameters and predictions of GxE interaction effects. Solar radiation intensity was identified in previous work (Jones et al., 2019) as having a significant effect on date of onset of stalk growth, likely a consequence of carbon source-sink dynamics. Such models would depend on all related trait parameter values being realistic for each G, which requires more experimental observations than were available in the dataset used in this study.

Resolving the uncertainties around G and E effects on RUE requires data recorded with great precision, as this analysis was hampered by data shortcomings – water stress, lodging, inadequate FIPAR measurements, and large sampling error in ADM yields. Experimental protocols should ensure that water, nutrition and biotic stresses are minimised and careful records should be kept of irrigation applications and lodging events; FIPAR should be measured at frequent thermal time intervals throughout the cropping season, and should immediately precede destructive sampling events; time-series sampling of biomass is also required, and should be done with care to reduce sampling errors; and RUEmax should be calculated using biomass samples taken between three and nine months' age.

In this work we assumed that the primary drivers of GxE interaction effects would be differential responses to temperature and radiation. It is however possible that other factors such as soil biotic factors could have played a role. Limitations in this dataset could be addressed with follow-up experimentation with greater control over soil biotic factors and improved experimental protocols. However, it is recommended that existing historical growth analysis datasets are used for future model development and testing.

The AS and DC models require separate execution environments for comparing the effects of 'species' parameters (those that are not G-specific), potentially adding complication to simulation workflows. Models should provide easily-defined G trait parameters for process-specific base temperatures and RUEo, for practical application in model-assisted breeding.

5. CONCLUSION

Three sugarcane models (DSSAT-Canegro, Mosicas and APSIM-Sugar) were calibrated using knowledge of G effects via phenotypic parameters published in a previous study. All three models reported favourable (and roughly equivalent) calibration statistics.

Observed genotype (G) by environment (E) differences in final harvest above-ground dry mass (ADM) yields were explained in terms of differences in seasonal average fractional photosynthetically-active radiation interception (FIPARa) and average seasonal radiation use efficiency (RUEa). While the models showed some skill in predicting G and E effects on ADM yield, none of the models reliably predicted ADM GxE interaction effects. All models greatly under-estimated variation in RUEa and ADM.

Cultivar CP88-1762 developed canopy cover faster, intercepted more radiation and out-yielded, R570 and N41 in Es with cool early-season conditions (Belle Glade and Pongola), while R570 outperformed the other Gs in the warm early season E (La Mare). This dynamic was not adequately captured by any of the models; although G and E effects on radiation interception were reasonably well-simulated, the models failed to predict the GxE interaction effects accurately. Models simulated RUEa G differences accurately overall for the 3-6 and 6-9 month biomass sampling periods, but not for seasonal RUEa. Data shortcomings prevented us from making strong conclusions regarding E or GxE interaction effects in RUEa, although the evidence indicates that models' abilities are weak in this regard.

Overall, the models failed to predict GxE interaction effects (for FIPARa, RUEa and ADM) on these Gs and Es accurately. The hypothesis, that using phenotypic data to determine model input trait parameters would result in accurate prediction of G and GxE interaction effects, was shown not to be true for these models and the dataset considered.

The key recommendations from this study are that sugarcane models must accommodate G-specific base temperature model inputs for germination and canopy development processes, and should include realistic linkages between carbon availability and canopy growth; these are anticipated to result in improved simulation of GxE interaction effects on growth and yield.

6. ACKNOWLEDGEMENTS

We would like to thank the International Consortium for Sugarcane Modelling (ICSM) and its constituent organisations for supporting this research, as well as the scientists and field and lab technicians of participating organisations. We are also grateful for the comments from two anonymous reviewers, whose insights resulted in considerable improvements to this paper.

7. REFERENCES

Bonsucro, 2017. Corbion launches its new PLA bioplastics produced from Bonsucro certified sugarcane [WWW Document]. URL https://www.bonsucro.com/corbion-launches-new-pla-bioplastics-produced-bonsucro-certified-sugarcane/ (accessed 1.22.20).

Coelho, A.P., Dalri, A.B., Fischer Filho, J.A., Faria, R.T. de, Silva, L.S., Gomes, R.P., 2020. Calibration and evaluation of the DSSAT/Canegro model for sugarcane cultivars under irrigation managements. Rev. Bras. Eng. Agrícola e Ambient.

de Mendiburu, F., 2019. agricolae: Statistical Procedures for Agricultural Research.

Dias, H.B., Inman-Bamber, G., Bermejo, R., Sentelhas, P.C., Christodoulou, D., 2019. New APSIM-Sugar features and parameters required to account for high sugarcane yields in tropical environments. Field Crop. Res. 235, 38–53. https://doi.org/10.1016/j.fcr.2019.02.002

Dias, H.B., Sentelhas, P.C., 2017. Evaluation of three sugarcane simulation models and their ensemble for yield estimation in commercially managed fields. Field Crop. Res. 213, 174–185. https://doi.org/10.1016/j.fcr.2017.07.022

Donaldson, R.A., Redshaw, K.A., Rhodes, R., Antwerpen, R. van, 2008. Season effects on productivity of some commercial South African sugarcane cultivars, I: Biomass and radiation use efficiency. Proc. South African Sugar Technol. Assoc. 517–527.

FAOSTAT, 2017. FAOSTAT Statistical Database [WWW Document]. URL http://www.fao.org/faostat/en/#data/QC (accessed 1.22.20).

Gomes, G.R., Rampon, D.S., Ramos, L.P., 2018. Production of Furan Compounds from Sugarcane Bagasse Using a Catalytic System Containing ZnCl2/HCl or AlCl3/HCl in a Biphasic System . J. Brazilian Chem. Soc. .

Guo, D., Westra, S., Peterson, T., 2017. Evapotranspiration: Modelling Actual, Potential and Reference Crop Evapotranspiration.

Hammer, G.L., Jordan, D.R., 2007. An integrated systems approach to crop improvement., in: Scale and Complexity in Plant Systems Research: Gene-Plant-Crop Relations. Springer-Verlag GmbH, Heidelberg, pp. 45–61.

Hoffman, N., 2017. Pot trial phenotyping to predict sugarcane genotype field performance with the Canegro Model. University of KwaZulu-Natal.

Hoffman, N., Singels, A., Patton, A., Jones, M.R., 2016. Pot trial phenotyping to predict genotype field performance with the Canegro model. Proc. South African Sugar Technol. Assoc. 149–153.

Hoffman, N., Singels, A., Patton, A., Ramburan, S., 2018. Predicting genotypic differences in irrigated sugarcane yield using the Canegro model and independent trait parameter estimates. Eur. J. Agron. 96, 13–21. https://doi.org/10.1016/j.eja.2018.01.005

Inman-Bamber, N., 1991. A growth model for sugar-cane based on a simple carbon balance and the CERES-Maize water balance. South African J. Plant Soil 1862, 37–41. https://doi.org/10.1080/02571862.1991.10634587

Inman-Bamber, N.G., 1994. Temperature and seasonal effects on canopy development and light interception of sugarcane. Field Crop. Res. 36, 41–51. https://doi.org/10.1016/0378-4290(94)90051-5

Inman-Bamber, N.G., Jackson, P.A., Stokes, C.J., Verrall, S., Lakshmanan, P., Basnayake, J., 2016. Sugarcane for water-limited environments: Enhanced capability of the APSIM sugarcane model for assessing traits for transpiration efficiency and root water supply. Field Crop. Res. 196, 112–123. https://doi.org/10.1016/j.fcr.2016.06.013

Inman-Bamber, N.G., Lakshmanan, P., Park, S., 2012. Sugarcane for water-limited environments: Theoretical assessment of suitable traits. Field Crop. Res. 134,

95–104. https://doi.org/10.1016/j.fcr.2012.05.004

Jones, M.R., 2013. Incorporating the Canegro sugarcane model into the DSSAT v4 Cropping System Model framework. University of KwaZulu-Natal, Pietermaritzburg.

Jones, M.R., Singels, A., 2018. Refining the Canegro model for improved simulation of climate change impacts on sugarcane. Eur. J. Agron. https://doi.org/10.1016/j.eja.2017.12.009

Jones, M.R., Singels, A., Chinorumba, S., Patton, A., Poser, C., Singh, M., Martiné, J.F., Christina, M., Shine, J., Annandale, J., Hammer, G., 2019. Exploring process-level genotypic and environmental effects on sugarcane yield using an international experimental dataset. Field Crop. Res. 244, 107622. https://doi.org/10.1016/j.fcr.2019.107622

Jones, M.R., Singels, A., Thorburn, P., Marin, F., Martine, J.F., Chinorumba, S., Viator, R., Nunez, O., 2014. Evaluation of the DSSAT-Canegro model for simulating climate change impacts at sites in seven countries. Proc. S. Afr. Sugar Technol. Assoc. 87, 323–329.

Jovanovic, N.Z., Annandale, J.G., 1998. Measurement of radiant interception of crop canopies with the LAI-2000 plant canopy analyzer. South African J. Plant Soil 15, 6–13. https://doi.org/10.1080/02571862.1998.10635107

Keating, B.A., Robertson, M.J., Muchow, R.C., Huth, N.I., 1999. Modelling sugarcane production systems I. Development and performance of the sugarcane module. Field Crop. Res. 61, 253–271. https://doi.org/10.1016/S0378-4290(98)00167-1

Luo, J., Que, Y., Zhang, H., Xu, L., 2013. Seasonal Variation of the Canopy Structure Parameters and Its Correlation with Yield-Related Traits in Sugarcane. Sci. World J. 2013, 801486. https://doi.org/10.1155/2013/801486

Marin, F.R., Jones, J.W., Royce, F., Suguitani, C., Donzeli, J.L., Pallone Filho, W.J., Nassif, D.S.P., 2011a. Parameterization and evaluation of predictions of DSSAT/CANEGRO for Brazilian sugarcane. Agron. J. 103, 304–315.

Marin, F.R., Jones, J.W., Royce, F., Suguitani, C., Donzeli, J.L., Pallone Filho, W.J., Nassif, D.S.P., 2011b. Parameterization and evaluation of predictions of DSSAT/CANEGRO for Brazilian sugarcane. Agron. J. 103, 304–315.

Marin, F.R., Thorburn, P.J., Nassif, D.S.P., Costa, L.G., 2015. Sugarcane model intercomparison: Structural differences and uncertainties under current and potential future climates. Environ. Model. Softw. 72, 372–386. https://doi.org/10.1016/j.envsoft.2015.02.019

Martiné, J.-F., Siband, P., Bonhomme, R., 1999. Simulation of the maximum yield of sugar cane at different altitudes: effect of temperature on the conversion of radiation into biomass. Agronomie 19, 3–12.

Martiné, J.-F., Todoroff, P.R.I., 2004. Le modèle de croissance mosicas et sa plateforme de simulation simulex: état des lieux et perspectives. Rev. Agric. Sucrière l'Ile Maurice 80 LB-U1, 133–147.

Robertson, M.J., Wood, A.W., Muchow, R.C., 1996. Growth of sugarcane under high input conditions in tropical Australia. I. Radiation use, biomass accumulation and partitioning. Field Crop. Res. 48, 11–25.

https://doi.org/https://doi.org/10.1016/0378-4290(96)00041-X

Sexton, J., Everingham, Y.L., Inman-Bamber, G., 2017. A global sensitivity analysis of cultivar trait parameters in a sugarcane growth model for contrasting production environments in Queensland, Australia. Eur. J. Agron. 88, 96–105. https://doi.org/10.1016/j.eja.2015.11.009

Sinclair, T.R., Muchow, R.C., 1999. Radiation Use Efficiency, in: Sparks, D.L.B.T.-A. in A. (Ed.), . Academic Press, pp. 215–265. https://doi.org/https://doi.org/10.1016/S0065-2113(08)60914-1

Singels, A., 2014. Crop Models. Sugarcane Physiol. Biochem. Funct. Biol., Wiley Online Books. https://doi.org/doi:10.1002/9781118771280.ch20

Singels, A., Bezuidenhout, C.N., 2002. A new method of simulating dry matter partitioning in the Canegro sugarcane model. Field Crop. Res. 78, 151–164. https://doi.org/10.1016/S0378-4290(02)00118-1

Singels, A., Donaldson, R.A., 2000. A simple model of unstressed sugarcane canopy development. Proc. S. Afr. Sugar Technol. Assoc. 74, 151–154.

Singels, A, Jones, M.R., Porter, C.H., Smit, M.A., Kingston, G., Marin, F., Chinorumba, S., Jintrawet, A., Suguitani, C., van den Berg, M., 2010a. The DSSAT4.5 Canegro model: A useful decision support tool for research and management of sugarcane production, in: Proceedings of the International Society of Sugar Cane Technologists.

Singels, A, Smit, M.A., Butterfield, M.K., Van Heerden, P.D.R., Van Den Berg, M., 2010b. Identifying quantitative trait alleles for physiological traits in sugarcane: an exploratory study, in: Proc. Int. Soc. Sugar Cane Technol.

Singels, A, van den Berg, M., Smit, M.A., Jones, M.R., van Antwerpen, R., 2010c. Modelling water uptake, growth and sucrose accumulation of sugarcane subjected to water stress. Field Crop. Res. 117, 59–69. https://doi.org/10.1016/j.fcr.2010.02.003

Thorburn, P., Biggs, J., Jones, M.R., Singels, A., Marin, F., Martine, J.F., Chinorumba, S., Viator, R., Nunez, O., 2014. Evaluation of the APSIM-Sugar model for simulating sugarcane yield at sites in seven countries: initial results. Proc. S. Afr. Sugar Technol. Assoc. 87, 318–322.

Wilkens, P.W., Hoogenboom, G., Porter, C.H., Jones, J.W., Uryasev, O., 2004. Decision Support System for Agrotechnology Transfer Version 4.0. Volume 2. DSSAT v4: Data Management and Analysis Tools. University of Hawaii, Honolulu, HI.

Zhou, M., 2013. Conventional Sugarcane Breeding in South Africa: Progress and Future Prospects. Am. J. Plant Sci. 04, 189–197. https://doi.org/10.4236/ajps.2013.42025